Spin reorientation and crystal field in a $ErFe_{10.5}Mo_{1.5}$ single crystal

1998 J. Phys.: Condens. Matter 10 1403

(http://iopscience.iop.org/0953-8984/10/6/023)

J. Phys.: Condens. Matter **10** (1998) 1403–1411. Printed in the UK PII: S0953-8984(98)88887-5

Spin reorientation and crystal field in a $ErFe_{10.5}Mo_{1.5}$ single crystal

B García-Landa†, D Gignoux‡¶, R Vert‡, D Fruchart§ and R Skolozdra‖

† Departamento de Física de la Materia Condensada e Instituto de Ciencia de Materiales de Aragón, Facultad de Ciencias, Universidad de Zaragoza-CSIC, 50009 Zaragoza, Spain
‡ Laboratoire de Magnétisme Louis Néel, CNRS, B.P. 166, 38042 Grenoble Cedex 9, France
§ Laboratoire de Cristallographie, CNRS, B.P. 166, 38042 Grenoble Cedex 9, France
‖ Chemistry Department, I. Franco University, 29000 Lviv, Ukraine

Received 31 October 1997

Abstract. Magnetization measurements performed on a single crystal of the tetragonal ferrimagnetic compound $ErFe_{10.5}Mo_{1.5}$ are presented together with their quantitative analysis. Between $T_C = 380$ K and a spin reorientation temperature $T_{SR} = 53$ K, the spontaneous magnetization is along the crystallographic $\boldsymbol{c}$ direction. Below T_{SR} the spontaneous magnetization progressively shifts away from $\boldsymbol{c}$ and is directed between this axis and the [100] direction. The results are rather well accounted for by considering the iron sublattice characteristics measured on a $YFe_{10.5}Mo_{1.5}$ single crystal and diagonalising the rare earth Hamiltonian through a system of coupled equations. A set of crystalline electric field (CEF) parameters and Er–Fe exchange field coefficient is proposed. It is shown that the spin reorientation does not come from a competition between iron anisotropy and the effect of the second order CEF parameter acting on the rare earth, as is frequently observed in this type of compounds. It results rather from the interaction between (i) the effect of these two contributions both of which favour the $\boldsymbol{c}$ axis, and (ii) that of the fourth order CEF terms, in particular B_4^0, which favour an intermediate direction of magnetization. The relative importance of this latter contribution is greatest at low temperature.

1. Introduction

The $RFe_{10.5}Mo_{1.5}$ alloys (R = rare earth) belong to the family of compounds which have the tetragonal $ThMn_{12}$-type structure (space group I4/mmm). Whereas RFe_{12} compounds do not exist, this phase can be stabilized by replacing some of the iron atoms by a small amount of other elements such as Ti, V, Cr, Mn, Mo, W, Re, Al, Si (Li and Coey 1993); for molybdenum, for example, $RFe_{12-x}Mo_x$ compounds can be obtained for $0.5 \leqslant x \leqslant 3$. These materials are of special interest because their hydride, nitride and carbide interstitials have potential magnetic properties for permanent magnet applications. The magnetic phase diagrams of the $RFe_{10.5}Mo_{1.5}$ series have been determined from magnetic measurements on oriented powders (Tomey *et al* 1995). As shown in figure 1 these compounds exhibit a large variety of behaviours, in particular spin reorientations, which are the result of the interplay of the rare earth and iron anisotropies together with a large antiparallel exchange coupling between the rare earth and iron spins. The main characteristics of these diagrams can be qualitatively accounted for by considering that : (i) the magnetocrystalline anisotropy

¶ Corresponding author. Fax: (33) 4 76 88 11 91, e-mail: gignoux@grmag.polycnrs-gre.fr.

0953-8984/98/061403+09$19.50

of the iron sublattice favours the c axis, (ii) the second order CEF parameter favours either the c axis or the basal plane for rare earths, with either a positive (Sm, Er, Tm) or negative (Ce, Pr, Nd, Tb, Dy, Ho) Stevens coefficient α_J, respectively. In fact this picture is simplified, in particular with Er we should have the spontaneous magnetization along c at any temperature, whereas a spin reorientation is observed around 53 K. Below this temperature magnetization measurements on oriented powder (Tomey *et al* 1995, Skolozdra *et al* 1995) as well as neutron diffraction experiments (Tomey *et al* 1994), show that the magnetization is directed between c and the basal plane.

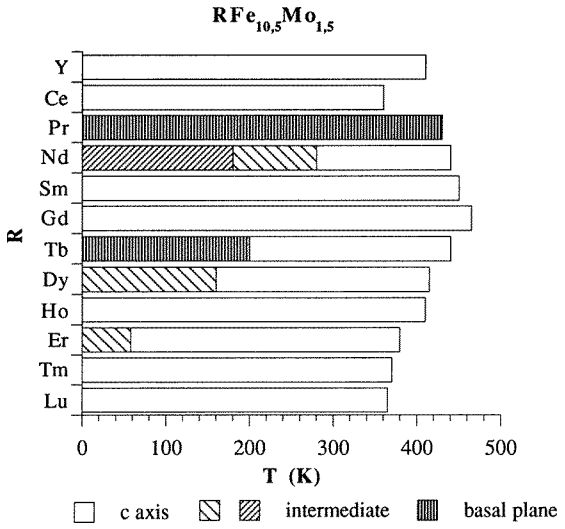

Figure 1. Magnetic phase diagram of the $RFe_{10.5}Mo_{1.5}$ compounds.

Magnetic measurements on a $ErFe_{10.5}Mo_{1.5}$ single crystal were briefly reported in a previous publication (García-Landa *et al* 1996). The purpose of this paper is to present in more detail the magnetization measurements on this single crystal, together with their quantitative analysis taking into account the different contributions to the total magnetic energy of the system.

2. Experimental results

The crystal has been prepared by the Czochralski technique in a cold crucible induction furnace. From the ingot, a crystal of about 3 mm^3 has been extracted. The purity of the sample has been checked using x-ray diffraction. Magnetization was measured by the extraction method in fields up to 10 T at temperatures ranging from 4 to 300 K along the [100], [110] and [001] symmetry directions. The crystal was oriented using the x-ray Laue diffraction technique.

Figure 2 shows the magnetization as a function of the internal field (applied field corrected for demagnetising field effects) measured at different temperatures along the three symmetry axes. At 4, 20 and 40 K, a non-zero spontaneous magnetization is observed along the three directions of measurement, showing that the magnetization is not along one of these axes. From the relative values of these spontaneous magnetizations it can be easily concluded that magnetization lies within the {010} plane, i.e. inbetween the [100] and [001] directions. The angle, θ, that the magnetization makes with the [001] axis has been

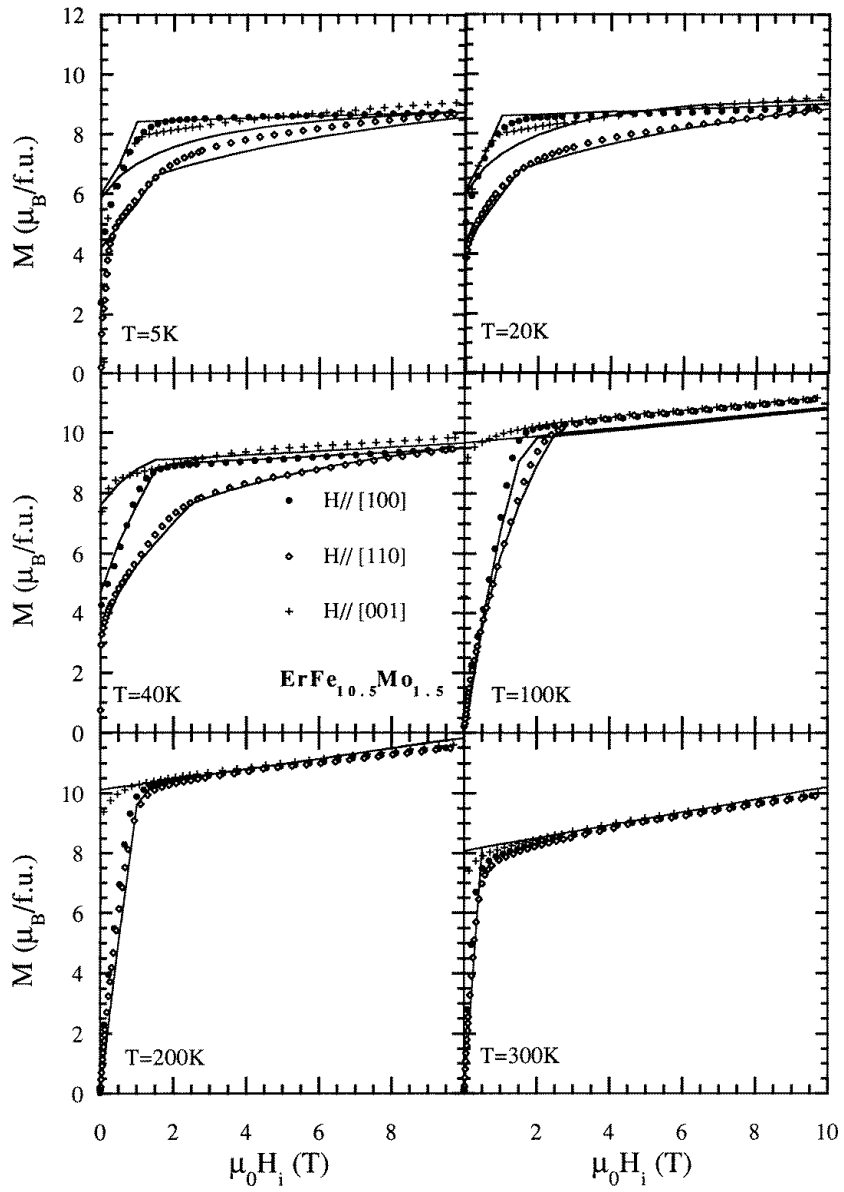

Figure 2. $ErFe_{10.5}Mo_{1.5}$: magnetization as a function of the internal field (applied field corrected for demagnetising field effects) measured at different temperatures along the three symmetry axes [100], [110] and [001]. Full lines are the calculated variations.

determined, and its thermal variation is shown in figure 3. At low temperatures, θ reaches about 45°, and when the temperature increases to the spin reorientation (SR) temperature $T_{SR} = 53 \pm 2$ K, it decreases to zero. Above T_{SR} the spontaneous magnetization is parallel to $\boldsymbol{c}$, as shown in figure 2, where magnetization curves at 100, 200 and 300 K are shown.

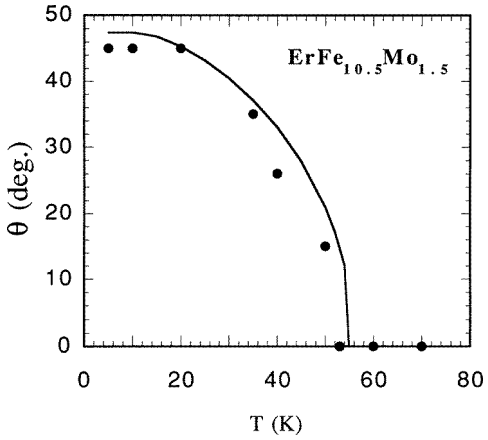

Figure 3. $ErFe_{10.5}Mo_{1.5}$: angle θ between the spontaneous magnetization and the $\boldsymbol{c}$ axis as a function of temperature. Full line is the calculated variation.

3. Analysis

As quoted in the introduction, the intermediate direction of magnetization observed at low temperature cannot be simply explained considering that both the Fe sublattice anisotropy and the second order CEF parameter acting on erbium favour the $\boldsymbol{c}$ axis. This last assumption is deduced from the magnetic properties of other compounds of the series and by considering that the sign of the second order CEF parameter follows that of the Stevens multiplicative factor α_J (Hutchings 1964). In order to account for the observed properties a more quantitative analysis is needed. For that purpose we used an approach similar to that which allowed a satisfactory account for the magnetic properties of the isomorphous $DyFe_{11}Ti$ compound, where a spin reorientation was also observed (Hu *et al* 1990). Within the molecular field approximation we have to solve a system of coupled equations for both the iron and rare earth sublattice magnetizations. In the following, these magnetizations per formula unit are defined as $\boldsymbol{M}_{Fe} = 10.5\langle \boldsymbol{m}_{Fe}\rangle$ and $\boldsymbol{M}_R = \langle \boldsymbol{m}_R\rangle$, where $\langle \boldsymbol{m}_{Fe}\rangle$ and $\langle \boldsymbol{m}_R\rangle$ are the average moment on iron and rare earth atoms, respectively. The magnetic interactions in the system are: (i) the dominant Fe–Fe exchange, which is the main contribution to the molecular field acting on the iron ions, (ii) the intersublattice R–Fe coupling and (iii) the weak indirect exchange interaction between localized R moments.

The energy of the iron sublattices per formula unit can be written as

$$E_{Fe} = E_a^{Fe} + E_{app} + E_{RFe} + E_{FeFe} \tag{1}$$

where

$$E_a^{Fe} = K_1 \sin^2\theta_{Fe} + K_2 \sin^4\theta_{Fe} \tag{2}$$

is the Fe sublattice anisotropy limited to the fourth order term, θ_{Fe} being the angle between the Fe sublattice magnetization and the $\boldsymbol{c}$ axis. The energy under the applied field is given by

$$E_{app} = -\mu_0 \boldsymbol{M}_{Fe} \boldsymbol{H}_i \tag{3}$$

where $\boldsymbol{H}_i$ is the internal field, i.e. the applied field corrected for demagnetising field effects.

$$E_{RFe} = -n_{RFe} N \boldsymbol{M}_R \boldsymbol{M}_{Fe} = -\gamma n_{RFe}^S N \boldsymbol{M}_R \boldsymbol{M}_{Fe} \tag{4}$$

is the exchange energy between the rare earth and iron sublattices. In this expression, $\gamma = 2(g_J - 1)/g_J$ and N, n_{RFe} and $n^S_{RFe}(< 0)$ are the number of formula units per unit volume, the molecular field coefficient and the negative molecular field coefficient between spin magnetizations, respectively (Gignoux and Schmitt 1995). In this notation, n^S_{RFe} corresponds to the n_{RFe} coefficient used by Hu *et al* (1990). The interest of using this former coefficient is that, in a given series, due to the similarity of the rare earth band structures, it is usually assumed to be almost constant.

$$E_{FeFe} = -\frac{1}{2} n_{FeFe} \boldsymbol{M}^2_{Fe} N \tag{5}$$

is the exchange energy within the iron sublattice. We will see latter that it is not necessary to consider this term is our calculation.

Whereas the iron energy is treated phenomenologically, for the rare earth we can consider the following Hamiltonian acting on the ground state multiplet of the Er3+ ion

$$\mathcal{H}_R = \mathcal{H}_{CEF} + (\gamma n^S_{RFe} N \boldsymbol{M}_{Fe} + \mu_0 \boldsymbol{H}_i) g_J \mu_B \boldsymbol{J} \tag{6}$$

where

$$\mathcal{H}_{CEF} = B^0_2 O^0_2 + B^0_4 O^0_4 + B^4_4 O^4_4 + B^0_6 O^0_6 + B^4_6 O^4_6 \tag{7}$$

is the CEF contribution in tetragonal symmetry. In this expression, the B^m_l terms are the CEF parameters whereas the O^m_l terms are the Stevens equivalent operators (Hutchings 1964). The second and third terms of equation (6) are the R–Fe exchange energy and the energy due to the internal field, respectively. In equation (6) we have neglected the exchange energy within the rare earth sublattice which is, as mentioned above, one order of magnitude smaller than the other exchange terms.

At a given temperature, the free energy of the rare earth sublattice is calculated as $F_R = -k_B T \ln Z_R$, where k_B is the Boltzmann constant and Z_R is the partition function. The total free energy can then be expressed as

$$E_{Tot} = E_{Fe} + F_R - E_{RFe} \tag{8}$$

where the last term is introduced because the R–Fe exchange energy has been considered twice, first in the Fe energy and second in the R Hamiltonian. This energy becomes :

$$E_{Tot} = -k_B T \ln Z_R + K_1 \sin^2\theta_{Fe} + K_2 \sin^4\theta_{Fe} - \mu_0 \boldsymbol{M}_{Fe} \cdot \boldsymbol{H}_i + E_{FeFe}. \tag{9}$$

In our analysis, the phenomenological parameters describing the spontaneous iron sublattice magnetic behaviour at each temperature (anisotropy constants and spontaneous magnetization) were initially taken as those measured on a $YFe_{10.5}Mo_{1.5}$ single crystal (Vert *et al* 1998). As we will see later, they were subsequently adjusted, in order to more accurately describe the experimental results. Moreover a superimposed susceptibility of the iron magnetization was taken into account at each temperature. It was considered as equal to that measured in the yttrium based single crystal.

For a given set of CEF parameters and R–Fe exchange field coefficient, at the applied field and temperature considered, the magnetic state of the system was determined as follows. For any direction of the iron sublattice magnetization the rare earth Hamiltonian is diagonalized, and the eigenvalues E_i and eigenvectors $|\psi_i\rangle$ are obtained. The equilibrium direction for the iron sublattice magnetization $(\theta^*_{Fe}, \phi^*_{Fe})$, is determined by finding the minimum of the free energy (9) of the system (θ and ϕ are the standard spherical angles). If several minima appear the lowest one is chosen. Note that the solution is independent of the E_{FeFe} energy term, which remains constant during the procedure. Thus this term was not considered in the analysis. At the equilibrium, the magnetic moment of the $RFe_{10.5}Mo_{1.5}$

system results from the addition of the contributions arising from the iron and the rare earth sublattices.

Due to the large number of parameters involved in the calculation we did not find a unique solution. Several sets of parameters give acceptable fits to the results. Among them we have retained that which leads to the best fits of the experimental data. The calculated variations of magnetization are reported in full lines in figure 2. The B_l^m and corresponding A_l^m CEF parameters are reported in table 1. The R–Fe exchange field coefficient is $n_{RFe}^S = -142\mu_0$. The thermal variations of the K_1 and K_2 anisotropy constants on the one hand, and of the iron sublattice magnetization M_{Fe} in zero internal field on the other hand, retained for the calculation are compared with those obtained on the $YFe_{10.5}Mo_{1.5}$ single crystal in figures 4 and 5 respectively. The values M_{Fe} are larger than those measured on the single crystal but slightly smaller than those measured on an oriented powder of $YFe_{10.5}Mo_{1.5}$ (Tomey 1994). The variation of K_1 almost follows that of the Y-based single crystal, the latter being slightly larger at low temperature.

The set of retained parameters gives a rather good account for the magnetization curves along the three selected symmetry axes in a large range of temperature. The calculated thermal variation of the angle θ between the total magnetization and the $\boldsymbol{c}$ axis within the plane containing the [100] and [001] directions is reported in figure 3. It fits well with the experimental values. Let us quote that, during this reorientation process, the Er and Fe sublattice magnetizations never discard from collinearity by an angle larger than 1.3°.

Table 1. Crystal field B_l^m parameters (in K/ion) obtained in $ErFe_{10.5}Mo_{1.5}$. The associated A_l^m parameters (in $K a_0^{-l}$/ion) are also reported ($A_l^m = B_l^m \theta_l \langle r^l \rangle$) where the θ_l are the Stevens factors (Hutchings 1964) and the $\langle r^l \rangle$ are obtained from Freeman and Desclaux (1979)).

B_2^0	B_4^0	B_4^4	B_6^0	B_6^4
-0.245×10^{-2}	0.218×10^{-3}	-0.365×10^{-2}	0.481×10^{-6}	0.192×10^{-5}
A_2^0	A_4^0	A_4^4	A_6^0	A_6^4
-1.35	3.87	-64.7	0.048	0.193

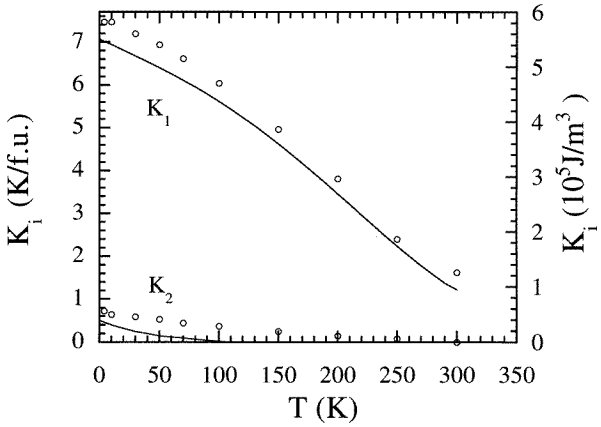

Figure 4. Thermal variations of the iron anisotropy constants K_1 and K_2. Full lines: variations used to fit the experiments on $ErFe_{10.5}Mo_{1.5}$. Circles: experimental values obtained on a $YFe_{10.5}Mo_{1.5}$ single crystal.

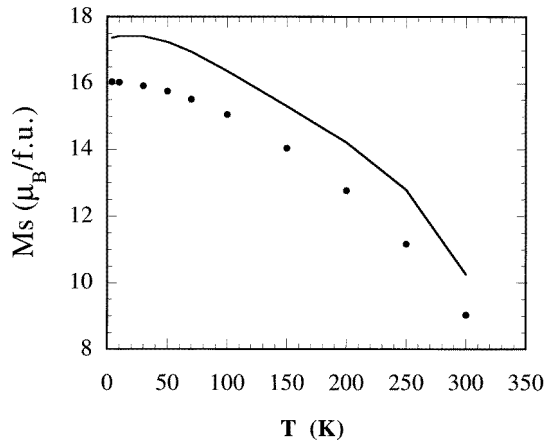

Figure 5. Thermal variation of the iron magnetization in zero applied field. Full line: variation used to fit the experiments on $ErFe_{10.5}Mo_{1.5}$. Circles: experimental values obtained on a $YFe_{10.5}Mo_{1.5}$ single crystal.

4. Discussion

A set of CEF and R–Fe exchange parameters has been found which gives a rather good account for the magnetic properties, in particular the spin reorientation, of $ErFe_{10.5}Mo_{1.5}$. Obviously it is possible to find other CEF parameters leading to similar results and it is not possible to assert that the proposed parameter set is the most definitive. Indeed it has been shown that in simpler systems, having the same symmetry but where only the rare earth is magnetic, the determination of a reliable set of CEF parameters is possible only from the quantitative interpretation of a large number of different experimental measurements (inelastic neutron diffraction, magnetization and susceptibility measurements on single crystals, specific heat...) (Gignoux and Schmitt 1997).

It is interesting to discuss the equilibrium magnetization direction using macroscopic anisotropy parameters within the strong exchange field approximation (compared to CEF effects) which implies that the rare earth moment has its maximum value $g_J \mu_B J$. Within the formalism presented by Franse and Radwanski (1993), the total anisotropy energy at 0 K in a compound with tetragonal symmetry can be expanded as

$$E_a = \kappa_2^0 P_2^0(\cos\theta) + \kappa_4^0 P_4^0(\cos\theta) + \kappa_4^4 P_4^4(\cos\theta)\cos 4\phi + \kappa_6^0 P_6^0(\cos\theta) + \kappa_6^4 P_6^4(\cos\theta)\cos 4\phi \quad (10)$$

where the κ_l^m and $P_l^m(\cos\theta)$ are the anisotropy coefficients and the Legendre functions, respectively. The former can be easily deduced from the Fe sublatice anisotropy constants and from the CEF parameters describing the anisotropy of the rare earth. It is then possible to determine the anisotropy energy for any direction of the total magnetization. This approach allows us to clearly identify the role of each of the CEF parameters. In figure 6 we have plotted E_a and each of its five components as a function of θ for $\phi = 0$, i.e. within the plane where the magnetization lies. We have also reported in figure 6 the total energy E_t obtained from the numerical calculation used for the fit. The absolute values of the E_a and E_t energies are not directly comparable as a large exchange contribution enters in E_t, so instead of E_t we have reported the quantity $\Delta E_t = E_t(\theta) - E_t(0) + E_a(0)$. The strong exchange field approximation leads to an easy direction of magnetization ($\theta = 42^\circ$)

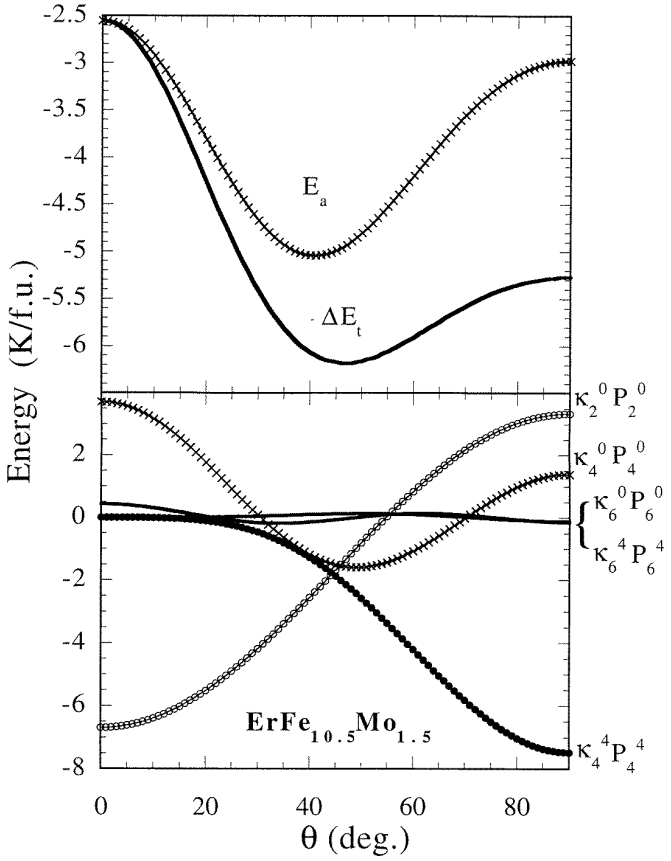

Figure 6. Upper part: variations of the magnetic energy in $ErFe_{10.5}Mo_{1.5}$ as a function of θ for $\phi = 0$ at $T = 5$ K obtained (i) by numerical calculations (ΔE_t) and (ii) using the high exchange field approximation (E_a). Lower part: plot of the different contributions to E_a.

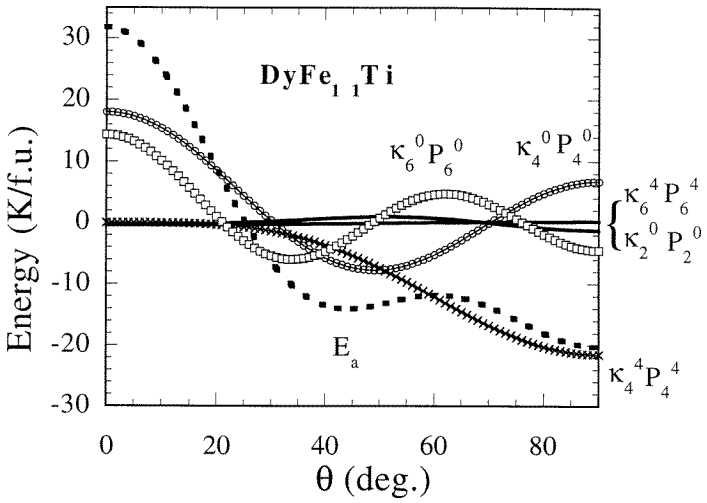

Figure 7. Variations of the anisotropy energy E_a at $T = 4$ K in $DyFe_{11}Ti$ and its different contributions as a function of θ for $\phi = 45^\circ$ within the strong exchange field approximation. The κ_l^m parameters were derived from Hu *et al* (1990).

close to that ($\theta = 47^\circ$) given by the more realistic numerical approach. From the different contributions to E_a we can see that, at low temperature, the intermediate direction arises from the fourth order terms of the CEF, in particular B_4^0 . When temperature increases, the progressive rotation towards the $\boldsymbol{c}$ axis originates from the faster decrease of the fourth order anisotropy coefficients, with respect to the second order one which favours the fourfold axis. Note that both the Fe anisotropy and B_2^0 favour the same anisotropy direction. Moreover, the corresponding A_2^0 parameter is found to be quite small for a uniaxial system, even smaller than that found in $DyFe_{11}Ti$ which was considered as especially weak (-32.3 K a_0^{-2}/ion).

The A_l^m CEF parameters proposed for $ErFe_{10.5}Mo_{1.5}$ are rather different from those determined in $DyFe_{11}Ti$ (Hu *et al* 1990). As a first assumption of our analysis we considered that in the Mo compounds, the CEF parameters were close to those of the Ti compounds, but found this to be unsuccessful. Finally it is worth noting that the CEF terms which are responsible for the spin reorientations in $ErFe_{10.5}Mo_{1.5}$ and $DyFe_{11}Ti$ are not the same. As stressed above, in the Er compound the sixth order terms are negligible whereas the fourth order ones play a crucial role. In the Dy compound, as can be seen in figure 7, it is the the sixth order term B_6^0 that plays a crucial role at low temperature, as it yields two close minima of the energy for $\theta = 90^\circ$ and an intermediate direction. It is the reason why, at low temperature, a first order transition occurs between these two states.

References

Franse J J M and Radwanski R J 1993 *Handbook of Magnetic Materials* vol 7, ed K H J Buschow (Amsterdam: Elsevier) 307–501

Freeman A J and Desclaux J P 1979 *J. Magn. Magn. Mater.* **12** 11–21

García-Landa B, Tomey E, Fruchart D, Gignoux D and Skolozdra R 1996 *J. Magn. Magn. Mater.* **157–158** 21–2

Gignoux D and Schmitt D 1995 *Handbook on the Physics and Chemistry of Rare Earths* vol 20, ed K A Gschneidner Jr and L Eyring (Amsterdam: North Holland) 293–424

Gignoux D and Schmitt D 1997 *Handbook of Magnetic Materials* vol 10, ed K H J Buschow (Amsterdam: Elsevier) 239–413

Hu B P, Li H S, Coey J M D and Gavigan J P 1990 *Phys. Rev.* B **41** 2221–8

Hutchings M T 1964 *Solid State Physics* (New York: Academic) **16** 227–73

Li H S and Coey J M D 1993 *Handbook of Magnetic Materials* vol 6, ed K H J Buschow (Amsterdam: North Holland) 1–83

Skolozdra R V, Tomey E, Gignoux D, Fruchart D and Soubeyroux J L 1995 *J. Magn. Magn. Mater.* **139** 65–76

Tomey E 1994 *PhD Thesis* University of Grenoble

Tomey E, Bacmann M, Fruchart D, Gignoux D, Miraglia S, Palacios E and Soubeyroux J L 1994 *IEEE Trans. Mag.* **30** 687–9

Tomey E, Bacmann M, Fruchart D, Soubeyroux J L and Gignoux D 1995 *J. Alloys Compounds* **231** 195–200

Vert R, Fruchart D, Gignoux D and Skolozdra R V 1997 *J. Magn. Magn. Mater.* **174** 117–20